Thickness-dependent photoelectrochemical property of tin disulphide nanosheets

Jiaxin Fang, Mengna Chen, Zhen Fang ✉

Key Laboratory of Functional Molecular Solids, Ministry of Education, Center for Nano Science and Technology, College of Chemistry and Materials Science, Anhui Normal University, Wuhu 241000, People's Republic of China
✉ *E-mail: fzfscn@mail.ahnu.edu.cn*

Published in Micro & Nano Letters; Received on 9th October 2016; Revised on 19th January 2017; Accepted on 24th January 2017

IV–VI group compounds are excellent candidates for optoelectronics. Here, a solvothermal controlled synthesis of SnS_2 nanosheets with different thickness is reported. The bandgap of nanosheets with thickness of 15 nm was estimated as 2.0 eV which is quite suitable for visible light harvesting. The nanosheets show about 180 times photoinduced current compare with the 35 nm nanosheets and fast response time of 4.9 ms, indicating that the SnS_2 nanosheets are potential materials for high-performance photodetectors.

1. Introduction: Two-dimensional (2D)-layered materials that featured with van der Walls interactions between neighbouring layers has inspired many research interests for the discovery of graphene [1–3]. As a counterpart of graphene, layered 2D metal chalcogenides have its own superiority including facile control synthesis and natural abundant [4–6]. Till now, many synthesis methods as well as the property of these ultrathin metal chalcogenides have been explored [7–10]. Among various 2D-layered chalcogenides, narrow bandgap IV−VI semiconductors are an earth-abundance, less toxicity, and chemical stability material with rich potential applications [11, 12]. For examples, GeS and GeSe nanosheets (NSs) synthesised by one-pot strategy is a promising light-adsorption layers in solar cell [13]. Ultrathin tin disulfide (SnS_2) NSs show an excellent lithium storage performance with highly reversible capacity [14]. Single-layer SnSe NSs have an improved photoresponse properties than the nanoflowers [15]. As an important IV−VI semiconductor, SnS_2 is an n-type semiconductor with bandgap of 2.18−2.44 eV. Besides using as anode materials in lithium ion battery, SnS_2 has potential application in photocatalysis and optoelectronics [16, 17]. However, the control synthesis of SnS_2 NSs with different thickness is still a challenge, and its photoelectrochemical property need further investigate.

2. Experimental section

2.1. Chemical synthesis: In a typical process, 1 mmol $SnCl_4{\cdot}5H_2O$ and 1 mmol sodium diethyldithiocarbamate were dissolved in 20 mL *N*, *N*-dimethyl formamide (DMF), respectively. The obtained solutions were mixed in a 50 mL Teflon-lined stainless steel autoclave and then heated at 200°C for 12 h. The products were collected by filtration and washed with ethanol and water for three times. After dried in vacuum at 60°C for 5 h, the SnS_2 NSs were obtained. If the reaction temperature was elevated to 220°C with other reaction conditions were retained, thick SnS_2 nanoplates (NPs) were the final products.

2.2. Charcterisations: X-ray diffraction (XRD; Bruker D8 ADVANCE) was used to determine the phase purities of the samples. The morphologies of the sample were observed by a field emission scanning electron microscopy (Hitachi S-4800 with 5 kV acceleration voltage). Diffuse reflection spectra were obtained using DUV-3700 UV-Vis-NIR spectrophotometer (Shimadzu).

2.3. Photoelectrochemical measurements: Three electrodes system was used to estimate photoelectrochemical response of the samples. A Pt wire and a standard Ag/AgCl electrode were taken as counter and reference electrodes, respectively. For preparation of working electrode, 6 mg sample (SnS_2 NSs or NPs dispersed in ethanol) were drop casting on a 2×2 cm^2 ITO glass. The electrolyte is 0.1 M Na_2SO_4 solution with pH = 7.5. Current–voltage curves and electrochemical impedance spectra were recorded by an electrochemical workstation (CHI 660E, Chenhua Co., Ltd.). A 500 W Xenon lamp (CHF-XM-500, Changtuo Technology Co., Ltd.) equipped with an ultraviolet cutoff filter ($\lambda > 400$ nm) was employed as light resource. The light intensity was 200 mW cm^{-2}.

3. Results and discussions: Fig. 1 is the XRD pattern of the NSs. The peaks can all be indexed as hexagonal phase SnS_2 (JCPDF No. 23-0677, $a = 3.65$ Å, $c = 5.90$ Å). High-intensity peaks located at 15.03° and 30.26° indicate the NSs have preferential growth direction along [001] zone axis. The layered crystal structure of SnS_2 is depicted in the inset image of Fig. 1, which clearly shows the obtained (001) exposed surface is the cleavage plane for layered SnS_2.

SEM is showed in Fig. 2 which illuminates uniform hexagonal sheet-like structure was obtained. Most NSs in Fig. 2*a* have side length of 150 nm. The thickness of the NSs is ∼15 nm as indicated in Fig. 2*b*. However, if the reaction temperature elevate to 220°C, the obtained hexagonal structure become inhomogeneity. Fig. 2*c* illustrates the side length of the products distribute from 100 to 200 nm and the thickness of the products increase to 35 nm (Fig. 2*d*). To differentiate the products obtained at different reaction temperature, the thicker NSs are denoted as nanoplates (NPs).

The UV-vis-NIR diffuse reflection spectra of the NSs and the NPs were investigated at room temperature. In Fig. 3*a*, the adsorption onset of the SnS_2 NSs and NPs is ∼800 and 670 nm. The bandgap (*Eg*) of the NSs and NPs were determined by relation formula between photon energy and optical adsorption

$$Ah\upsilon = B(h\upsilon - Eg)^n$$

where A is the adsorption coefficient, h is the Planck constant, υ is the frequency, B is a constant related to the material, and n is 1/2 for direct bandgap semiconductors, respectively. The curves of $(Ah\upsilon)^2$ versus $h\upsilon$ are plotted in Fig 3*b*. By extrapolating the linear portion of the curve to $\alpha h\upsilon = 0$, the *Eg* values of the SnS_2 NSs and NPs were estimated as 2.00 and 2.15 eV, which consist with the SnS_2 NSs reported by Yu *et al.* [17]. Compare with the NPs, obvious shrinkage of the bandgap is observed in the NSs. The shrinkage of bandgap come from the quantum confinement related effects in large 2D sheet-like particles [17, 18]. The narrowed bandgap of SnS_2 NSs is helpful to adsorption of visible light in a broaden range. An evidently enhanced light adsorption in the rage of

doi: 10.1049/mnl.2016.0654

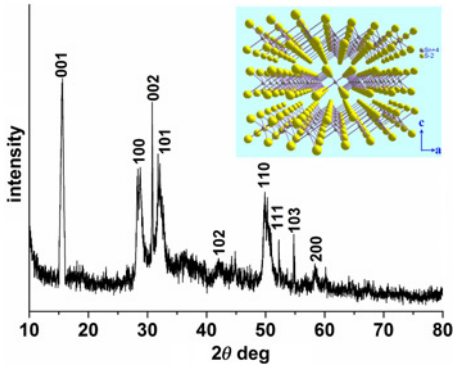

Fig. 1 *XRD of the obtained products. Inset image is the crystal structure of SnS_2 with layered structure observed from b-axis (Sn, silvery white balls; S, yellow balls)*

800–1000 nm in the NSs in Fig. 3*a* is also observed, it also helpful to adsorb the light in near infrared band.

To estimate the photoresponse and stability of the SnS_2 NSs, photocurrent versus time (*J*–*t*) curves were tested under chopped light irradiation. A typical n-type semiconductor photocurrent enhancement of the two samples are observed, indicating its photoanode feature. From the result showed in Fig. 3*c*, the dark currents of the NSs and NPs electrodes are nearly zero. In contrast, the currents of SnS_2 NSs increase quickly under irradiation and remain constant during the illumination time, and returns to its preillumination value when light off. This photocurrent response is stable at 10 μA in many light on/off cycles. As for SnS_2 NPs, the photocurrent is smaller than that of NSs obviously under identical condition, only 0.0545 μA photocurrent variations were observed.

The difference in photocurrent intensities between SnS_2 NSs and NPs could also be ascribed to the difference in their thickness. Firstly, compare with NPs, a 0.15 eV redshift of the bandgap for the SnS_2 NSs is a facility to uptake photons with lower energy. More carries can be excited for the NSs under the same irradiation intensity, which is helpful to increase the photocurrent. Secondly, in a layered structure semiconductor, covalent bond or van der Waals force is the main interaction inside or between layers, respectively. The calculation of layered GeS indicates that the majority of in-plane carriers are valence-band holes, while hopping is the out-of-plan carriers. The in-plane effective mass of holes is predominant carriers without irradiation, which result in anisotropy conductivity in layered GeS [19]. More experimental evidences had

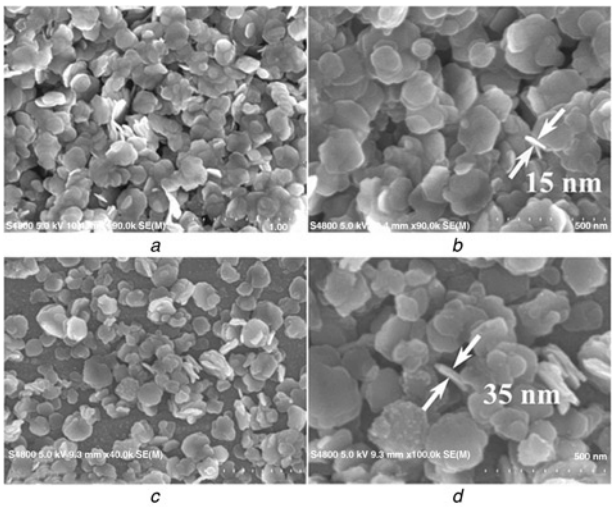

Fig. 2 *SEM images of the products obtained at 200°C (a and b) and 220°C (c and d)*

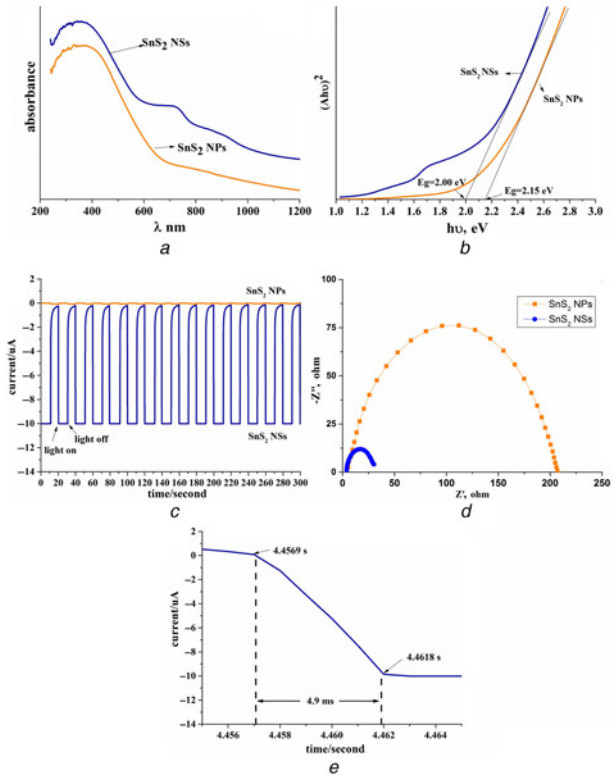

Fig. 3 *(a) UV-Vis-NIR diffuse reflectance adsorption spectra of SnS_2 NSs and NPs, (b) bandgap estimation of SnS_2 NSs and NPs. (c) Time-dependent photocurrents and cycle stability test of SnS_2 NSs and NPs measured with the potential bias of 0.13 V versus Ag/AgCl under chopped light irradiation. (d) The electrochemical impedance spectra of SnS_2 NSs and NPs. (e) Photoresponse time of SnS_2 NSs photoelectrode*

been provided by the layered GeSe NSs. Photosensitivity perpendicular to the layer is 3.5 times higher than parallel layers for dominated hopping transport [20]. Similar to the GeS and GeSe, perpendicular transport is the mainly carrier conduction method for layered SnS_2 under light illumination which will facilitate photoresponse. As the SnS_2 was drop casting on the ITO glass substrate, it is logical to conceive that most NSs were flat lay down on the substrate. The excited carriers will mainly transport in perpendicular of the NSs which result in a higher photoresponse. Thirdly, lower interfacial charge–transfer resistance is also responsible for enhanced photoresponse of thinner 2D NSs [21]. The electrochemical impedance spectra in Fig. 3*d* show that SnS_2 NSs have an interfacial charge–transfer resistance of 30 Ω, which is smaller than that of 207 Ω in NPs. The high-efficient carrier transport in the longitudinal direction results in a short photoresponse time [22–24]. As demonstrated in Fig. 3*e*, the saturation time of SnS_2 NSs photoelectrode under illumination is only 4.9 ms. From abovementioned reasons, it is concluded that the lower bandgap, layered structure as well as small thickness of the NSs will favour for the promotion of the PEC performance.

4. Conclusion: In conclusion, we demonstrated a solvothermal synthesis method for SnS_2 NSs. The PEC device of the NSs shows a high visible light response compare with thick NPs. This demonstrates that the 2D NSs of SnS_2 with narrow bandgap and high photoinduced carrier transport efficiency have application in water-splitting and photovoltaic cell.

5. Acknowledgments: This Letter was supported by Natural Science Foundation of China (NSFC grant nos. 21171007, 21671005) and the Programs for Science and Technology Development of Anhui Province (1501021019) is grateful.

6 References

[1] Duan X.D., Wang C., Pan A.L., *ET AL.*: 'Two-dimensional transition metal dichalcogenides as atomically thin semiconductors: opportunities and challenges', *Chem. Soc. Rev.*, 2015, **44**, (24), pp. 8859–8876

[2] Novoselov K.S., Jiang D., Schedin F., *ET AL.*: 'Two-dimensional atomic crystals', *Proc. Natl. Acad. Sci. USA*, 2005, **102**, (30), pp. 10451–10453

[3] Novoselov K.S., Geim A.K., Morozov S.V., *ET AL.*: 'Electric field effect in atomically thin carbon films', *Science*, 2004, **306**, (5696), pp. 666–669

[4] Lhuillier E., Pedetti S., Ithurria S., *ET AL.*: 'Two-dimensional colloidal metal chalcogenides semiconductors: synthesis, spectroscopy, and applications', *Acc. Chem. Res.*, 2015, **48**, (1), pp. 22–30

[5] Bouet C., Tessier M.D., Ithurria S., *ET AL.*: 'Flat colloidal semiconductor nanoplatelets', *Chem. Mater.*, 2013, **25**, (8), pp. 1262–1271

[6] Xu M., Liang T., Shi M., *ET AL.*: 'Graphene-like two-dimensional materials', *Chem. Rev.*, 2013, **113**, (5), pp. 3766–3798

[7] Yoon D., Seo B., Lee J., *ET AL.*: 'Facet-controlled hollow Rh_2S_3 hexagonal nanoprisms as highly active and structurally robust catalysts toward hydrogen evolution reaction', *Energy Environ. Sci.*, 2016, **9**, (3), pp. 850–856

[8] Rousseas M., Goldstein A.P., Mickelson W., *ET AL.*: 'Synthesis of highly crystalline SP2-bonded boron nitride aerogels', *ACS Nano*, 2013, **7**, (10), pp. 8540–8546

[9] Radisavljevic B., Radenovic A., Brivio J., *ET AL.*: 'Single-layer MoS_2 transistors', *Nat. Nanotechnol.*, 2011, **6**, (3), pp. 147–150

[10] Li H., Lu G., Wang Y., *ET AL.*: 'Mechanical exfoliation and characterization of single- and few-layer nanosheets of WSe_2, TaS_2, and $TaSe_2$', *Small*, 2013, **9**, (11), pp. 1974–1981

[11] Wang X., Liu B., Wang Q., *ET AL.*: 'Three-dimensional hierarchical $GeSe_2$ nanostructures for high performance flexible all-solid-state supercapacitors', *Adv. Mater.*, 2013, **25**, (10), pp. 1479–1486

[12] Deng Z., Cao D., He J., *ET AL.*: 'Solution synthesis of ultrathin single-crystalline SnS nanoribbons for photodetectors via phase transition and surface processing', *ACS Nano*, 2012, **6**, (7), pp. 6197–6207

[13] Vaughn D.D., Patel R.J., Hickner M.A., *ET AL.*: 'Single-crystal colloidal nanosheets of Ges and Gese', *J. Am. Chem. Soc.*, 2010, **132**, (43), pp. 15170–15172

[14] Zhai C., Du N., Zhang H., *ET AL.*: 'Large-scale synthesis of ultrathin hexagonal tin disulfide nanosheets with highly reversible lithium storage', *Chem. Commun.*, 2011, **47**, (4), pp. 1270–1272

[15] Li L., Chen Z., Hu Y., *ET AL.*: 'Single-layer single-crystalline SnSe nanosheets', *J. Am. Chem. Soc.*, 2013, **135**, (4), pp. 1213–1216

[16] Lei Y., Song S., Fan W., *ET AL.*: 'Facile synthesis and assemblies of flowerlike SnS_2 and In^{3+}-doped SnS_2: hierarchical structures and their enhanced photocatalytic property', *J. Phys. Chem. C*, 2009, **113**, (4), pp. 1280–1285

[17] Yu J., Xu C.Y., Ma F.X., *ET AL.*: 'Monodisperse SnS_2 nanosheets for high-performance photocatalytic hydrogen generation', *ACS Appl. Mater. Interfaces*, 2014, **6**, (24), pp. 22370–22377

[18] Jung Y., Zhou Y., Cha J.J.: 'Intercalation in two-dimensional transition metal chalcogenides', *Inorg. Chem. Front.*, 2016, **3**, (4), pp. 452–463

[19] Bletskan D.I., Madyar I.I., Mikulaninets S.V., *ET AL.*: 'Electrical and photoelectric properties of Ges layered crystals grown by different techniques', *Inorg. Mater.*, 2000, **36**, (6), pp. 544–550

[20] Xue D.-J., Tan J., Hu J.-S., *ET AL.*: 'Anisotropic photoresponse properties of single micrometer-sized GeSe nanosheet', *Adv. Mater.*, 2012, **24**, (33), pp. 4528–4533

[21] Fang Z., Hao S., Long L., *ET AL.*: 'The enhanced photoelectrochemical response of $SnSe_2$ nanosheets', *CrystEngComm*, 2014, **16**, (12), pp. 2404–2410

[22] Hu P., Wen Z., Wang L., *ET AL.*: 'Synthesis of few-layer GaSe nanosheets for high performance photodetectors', *ACS Nano*, 2012, **6**, (7), pp. 5988–5994

[23] Li L., Wu P., Fang X., *ET AL.*: 'Single-crystalline CdS nanobelts for excellent field-emitters and ultrahigh quantum-efficiency photodetectors', *Adv. Mater.*, 2010, **22**, (29), pp. 3161–3165

[24] Konstantatos G., Sargent E.H.: 'Nanostructured materials for photon detection', *Nat. Nano*, 2010, **5**, (6), pp. 391–400

doi: 10.1049/mnl.2016.0654